13th World Conference on Earthquake Engineering
Vancouver, B.C., Canada
August 1-6, 2004
Paper No. 206

OPTIMAL CRITICAL RESPONSE OF MULTI-STORY BUILDINGS TO RANDOM INPUT EXCITATIONS

G. GHODRATI AMIRI[1] and P. ASHTARI[2]

SUMMARY

Earthquake ground motions and the resultant responses of structures are very uncertain and random. Therefore, it is desirable to find the probable future excitation that can produce the worst and largest responses in the structures. A modified method of optimization in frequency domain is proposed to find the maximum response of multi-story buildings easier and faster than before. In this research, a stationary input excitation is found for shear model of buildings to maximize sum of the inter-story drifts as a design criterion. The input power (area of power spectral density (PSD) function) and the intensity (magnitude of PSD function) are fixed and the critical excitation is found under these constraints by solving a new optimization problem using Simpson integration. In the new method, optimization is performed numerically and the critical response is obtained efficiently during the less time by using very few steps to achieve the same accuracy. This method is presented for the structures with different modal frequencies. In addition, the large effect of the first modes relative to the higher modes, especially for narrow-band input excitations, is presented.

INTRODUCTION

In the recent seismic design procedures, a spectrum is found according to the past earthquakes. The structures designed by this design spectrum can really resist the past earthquakes but not certainly the future earthquakes maybe with completely different frequency content. For designing the important structures like power plants and tall buildings, reliability and safety are the most important parameters. So it is needed to obtain the worst and critical input excitation analytically and numerically regardless of the past earthquakes.
First of all, R.F. Drenick [1] introduced the concept of critical input excitations in time domain for structures. Shinozuka [2] expressed the same problem in the frequency domain and presented narrower upper bound of the maximum response. Up to now, lots of people have worked on the subject of critical input excitation. Recently, Takewaki [3] has developed a new critical excitation method for stationary inputs. He proposed a new constrained optimization problem in frequency domain by limiting the input power (area of power spectral density function) and the intensity (magnitude of PSD function). Authors in

---

[1] Associate Professor, Dept. of Civil Engineering, Iran University of Science & Technology, Tehran, IRAN
[2] Ph.D. Candidate, Dept. of Civil Engineering, Iran University of Science & Technology, Tehran, IRAN E-mail: ashtari@iust.ac.ir, Fax: (98-21) 745-4053

their last papers [4,5] introduced some exact and numeric methods of solving that optimization problem. In this research, it is tried to solve the optimization problem by a modified numeric method with a few steps to decrease the running time of computer program. This efficient method is so much useful specially for large structures.
Therefore, the essential part of random vibration theory of critical excitation optimization problem for stationary inputs is described briefly in the next section.

1- THEORY OF OPTIMIZATION PROBLEM OF CRITICAL EXCITATION

1-1- Random Vibration Theory

Consider an *n*-story building (Fig. 1), subjected to horizontal ground acceleration $\ddot{u}_g(t)$ that is a stationary Gaussian random process with zero mean. Taking Fourier transform from both sides of the *equation* of motion of the multi-storey building in time domain gives equation of motion in frequency domain as [6]

$$(-\omega^2\boldsymbol{M}+i\omega\boldsymbol{C}+\boldsymbol{K})U(\omega) = -\boldsymbol{Mr}\,\ddot{U}_g(\omega) \quad (1)$$

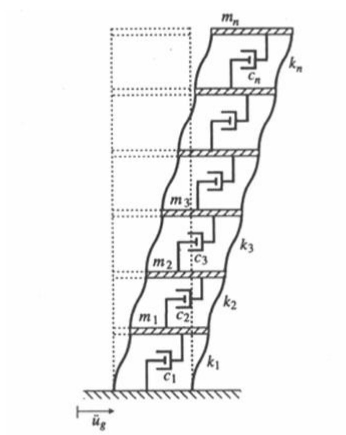

Fig. 1. n-*story shear building model subjected to horizontal base acceleration*

$\boldsymbol{M}$, $\boldsymbol{C}$ and $\boldsymbol{K}$ represent the system mass, viscous damping, stiffness matrices, respectively and $\boldsymbol{r} = \{1,\ldots,1\}^t$ represents the influence coefficient vector for transferring displacements to drifts. $\boldsymbol{U}(\omega)$ and $\ddot{U}_g(\omega)$ are the Fourier transforms of the horizontal floor displacement $u(t)$ and the horizontal input acceleration $\ddot{u}_g$(t), respectively. $\boldsymbol{C}$ is physical damping matrix or Rayleigh damping or generalized proportional damping [6]. Equation (1) can be reduced to the following form

$$\boldsymbol{A}U(\omega) = \boldsymbol{B}\ddot{U}_g(\omega) \quad (2)$$

Where

$$\boldsymbol{A} = (-\omega^2\boldsymbol{M}+i\omega\boldsymbol{C}+\boldsymbol{K}) \quad (3)$$

$$\boldsymbol{B} = -\boldsymbol{Mr} \quad (4)$$

Interstory drifts are defined as $d(t)=\{d_i(t)\}$ and their Fourier transforms as $\boldsymbol{D}(\omega) =\{\boldsymbol{D}_i(\omega)\}$. Then $\boldsymbol{D}(\omega)$ is related to $\boldsymbol{U}(\omega)$ as

$$\boldsymbol{D}(\omega)=\boldsymbol{TU}(\omega) \quad (5)$$

Where $\boldsymbol{T}$ is a constant transformation matrix consisting of –1, 1 and 0.

$$\boldsymbol{T}(i,i) = +1 \qquad : i=1,\ldots,n \quad (6)$$

$$\boldsymbol{T}(i,i\text{-}1) = -1 \qquad : i=2,\ldots,n \quad (7)$$

$\boldsymbol{T(i,j)=0} \qquad : j \neq i \;\; \& \;\; j \neq i-1$ (8)

Combining equations (2) and (5) leads to

$$\boldsymbol{D(\omega)=TA^{-1}B}\ddot{U}_g(\omega) \tag{9}$$

Where $\boldsymbol{H_D(\omega)=\{H_{Di}(\omega)\}}$ is the transfer complex frequency response function of the interstory drifts as

$$\boldsymbol{H_D(\omega)=TA^{-1}B} \tag{10}$$

$S_g(\omega)$ denotes the PSD function of the input $\ddot{u}_g(t)$. Using the random vibration theory, the mean square of the i[th] interstory drift can be computed from

$$E\left[d_i^2(t)\right]=\sigma_{D_i}^2=\int_{-\infty}^{+\infty}\left|H_{D_i}(\omega)\right|^2 S_g(\omega)\;d\omega=\int_{-\infty}^{+\infty}H_D(\omega)H_D(-\omega)\;S_g(\omega)\;d\omega \tag{11}$$

Taking the summation of all the variances of drifts as a displacement criterion gives

$$f=\sum_{i=1}^{n}\sigma_{Di}^2=\int_{-\infty}^{+\infty}F(\omega)\;S_g(\omega)\;d\omega \tag{12}$$

Where

$$F(\omega)=\sum_{i=1}^{n}\left|H_{Di}(\omega)\right|^2 \tag{13}$$

1-2- Shape of the F-function ($F(\omega)$)

Since the integration of $F(\omega)$, means the area under its curve, is the most important part of the objective function, shape of the *F*-function becomes important in the critical excitation optimization. *F*-function generally has up to n peaks near modal frequencies for an n-DOF system. $F(\omega)$ is a function of dynamic parameters of the structure like modal frequencies and dampings. In the figure 2, three models with different modal parameters are shown. In the figure 3, different shapes of $F(\omega)$ for these 2-DOF systems have been shown. If the frequency of the first and the second mode are far from each other, *F*-function has two peaks like figure 3(a). If these two frequencies are near together, *F*-function has two peaks besides together like figure 3(b). In the figure 3(c), two modal frequencies are so much near that produce only one peak in the *F*-function

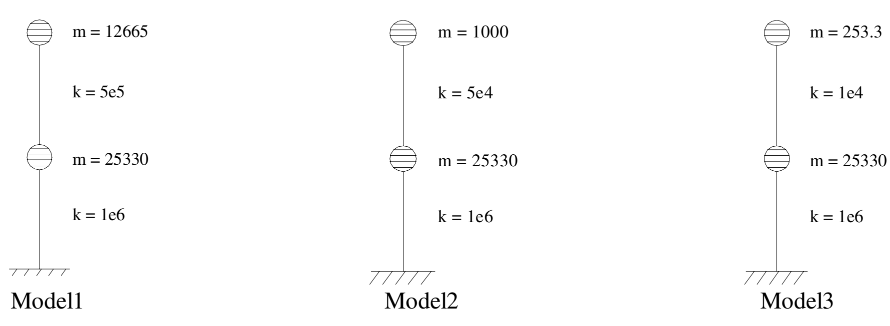

Fig. 2. *Three 2-DOF systems*

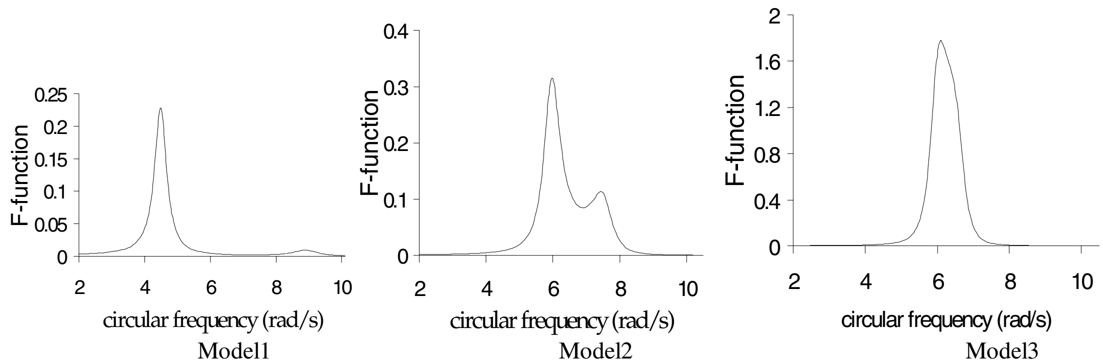

(a) (b) (c)

Fig. 3. *F-function for 2-DOF systems*

As seen in figure 3, the peaks of F-function are higher in the first modes and become lower in the higher modes. As a generalization for 2-DOF systems, a frequency range ($\Delta\hat{\omega}$) around the first mode can be found that F-function value is higher than the peak value of the second mode. In the figure 4, this frequency range is shown between $\hat{\omega}_1$ and $\hat{\omega}_2$ for the model1 and model2. $\Delta\hat{\omega}$ for model1 and model2 with $\xi = 0.05$ is equal to 2.258 and 0.898 rad/sec, respectively.

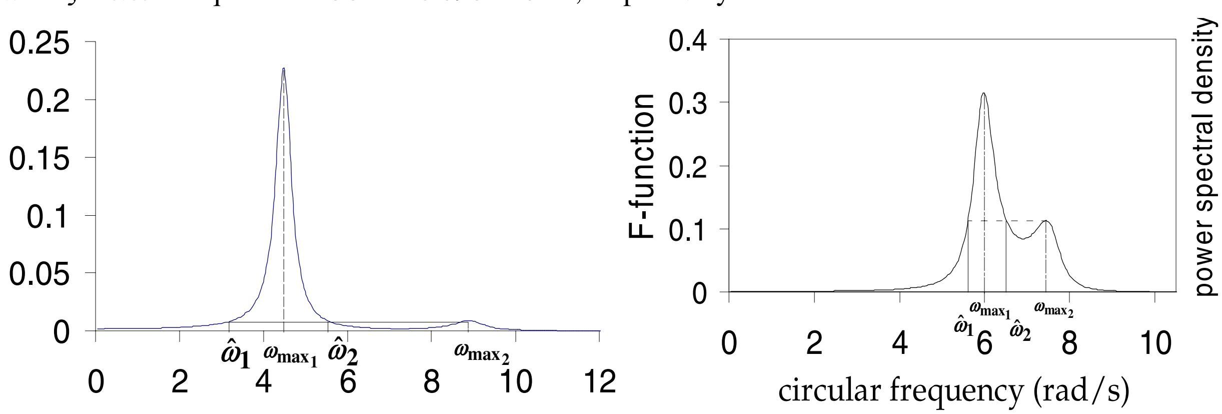

Model1 Model2

Fig. 4. *Higher range of the first mode*

2- INTRODUCING THE OPTIMIZATION PROBLEM

Referring to Takewaki [3], for finding the critical excitation, an optimization problem of the general case can be expressed as

$$Max\ f = \sum_{i=1}^{n} \sigma_{Di}^2 = \int_{-\infty}^{+\infty} F(\omega) S_g(\omega)\ d\omega \tag{14}$$

Subject to

$$\int_{-\infty}^{+\infty} S_g(\omega)\ d\omega \le \bar{S} \qquad (\bar{S} = \ given\ \ Power\ \ limit) \tag{15}$$

$$S_g(\omega) \le \bar{s} \qquad (\bar{s} = given\ \ PSD\ \ amplitude\ limit) \tag{16}$$

As previously indicated, F-function generally has up to n peaks near modal frequencies for an n-DOF system. So the input excitation should be divided into some pieces to resonate the different modes. In each piece, because of maximization, S_{gi} equals to maximum intensity ($\bar{s}$) for all the ω's. So the shape of

input excitation becomes rectangular. Then only the frequency content should be obtained. Therefore, the start and the end circular frequency of rectangles should be specified as the result of optimization.
Because of the rectangular frequency bands, the constraints of optimization problem of the general case can be expressed as

$$\sum_{i=1}^{n} S_{g_i} \Delta\omega_i \leq \overline{S} : i = 1,\ldots,n \tag{17}$$

$$0 \leq S_{g_i} \leq \overline{s} : i = 1,\ldots,n \tag{18}$$

$$0 \leq \Delta\omega_i : i = 1,\ldots,n \tag{19}$$

This optimization problem is a nonlinear constrained one with boundary values. Regarding to that all the S_{gi}'s are equal to maximum intensity ($\overline{s}$), the relation (17) could be simply written as

$$\sum_{i=1}^{n} \Delta\omega_i \leq \frac{\overline{S}}{\overline{s}} = \Delta\omega_{total} \tag{20}$$

$\Delta\omega_{total}$ (summation of frequency bandwidths) is pre-specified and equal to $\overline{S}/\overline{s}$. So only the optimal distribution of total band width in frequency domain is desirable.
As an example, we take a 2-DOF structure with the F-function as shown in figure 5. If we assume total bandwidth around the first mode, we reach to F-functions less than the peak value of the second mode (Fig. 5(a)). Therefore, for considering the greater F-functions, we should place a share of bandwidth around the second mode (Fig. 5(b)) dictated by a line named "Optimum line".

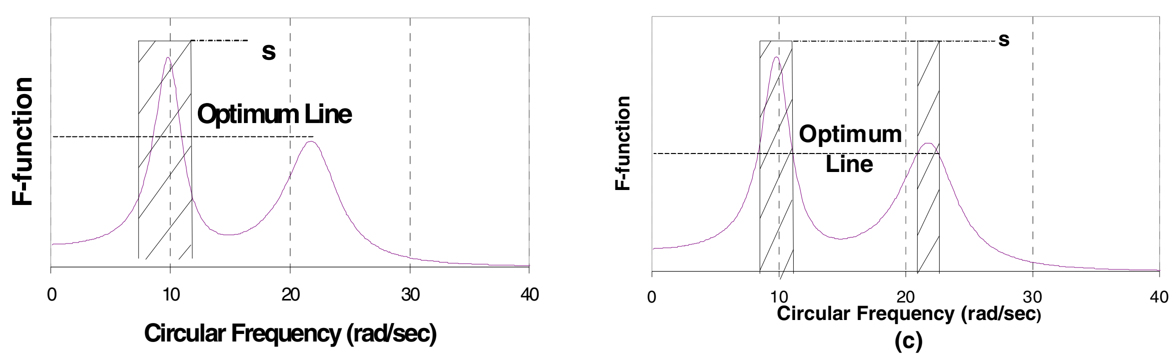

(a) *Nonoptimal* **(b)** *Optimal*

Fig. 5. *Comparison of optimal and non-optimal critical excitation of a 2DOF system*

Even in MDOF systems, a horizontal line named "Optimum Line" can be used (figure 6). Each horizontal line has one objective function value *(f)*. The "Optimum Line" is the horizontal line that gives the total frequency bandwidth equal to $\overline{S}/\overline{s}$. So it can be easily proved that all the circular frequencies at the ends of each rectangular band of all the modes have the same F-function value (figure 6).

$$F(\omega_{1\max}) = F(\omega^*_{1\max}) = F(\omega_{2\max}) = F(\omega^*_{2\max}) = \ldots \tag{21}$$

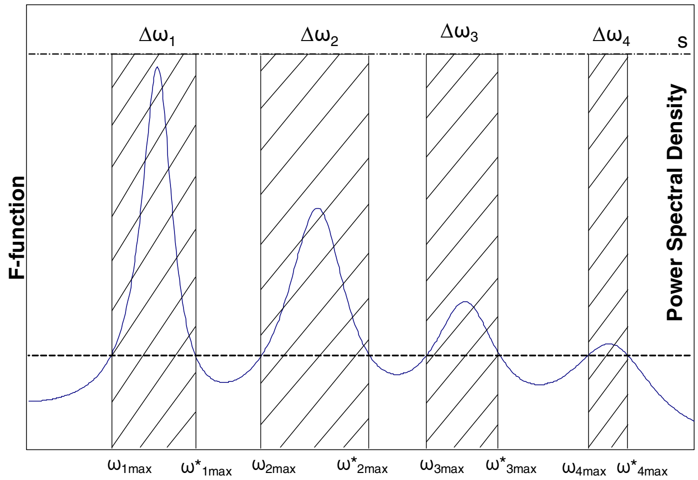

Fig. 6. *Schematic position of frequency bands of all the mode*

3- NUMERICAL OPTIMIZATION METHOD FOR FINDING CRITICAL EXCITATION

3-1- Ordinary Optimization Method

However, as introduced in the first papers of authors [4], the "Optimum Line" is a simple geometric solution. But finding the intersection point of F-function curve with a considered horizontal line can't be easily achieved. In other words, finding the start (and the end) frequencies of each rectangular frequency band is difficult: $\omega_{1\mathbf{max}}, \omega^*_{1\mathbf{max}}, \omega_{2\mathbf{max}}, \omega^*_{2\mathbf{max}}, \dots$.

To overcome this difficulty, a simple method of optimization was proposed by authors [5]. In this method, frequency range of F-function is divided into $\delta\omega$'s. The mid point of each $\delta\omega$ is founded, then F(ω) for all the start, end and mid points is calculated. So the area under F(ω) in each $\delta\omega$ can be computed using the quadratic approximation of Simpson method of integration

$$\delta A = \int_{\omega_1=\omega_i}^{\omega_2=\omega_i+\delta\omega} F(\omega)\ d\omega = \delta\omega\left[F(\omega_i) + 4F\left(\omega_i + \frac{\delta\omega}{2}\right) + F(\omega_i+\delta\omega)\right] \tag{22}$$

After finding the δA_i 's for all the $\delta\omega_i$'s, they are sorted in descending order $\delta A_1 \geq \delta A_2 \geq \delta A_3 \geq \dots$.

Now we have

$$\mathbf{max}\int F(\omega)\ d\omega = \sum_{1}^{[N]} \delta A_i + (N - [N])\ \delta A_{[N]+1} \tag{23}$$

Where $[N]$ is the round part of N

$$N = \frac{\overline{S}/\overline{s}}{\delta\omega} \tag{24}$$

By decreasing $\delta\omega$, δA_i 's decreases and the equation (23) is reduced to the simplified form with a good accuracy

$$\mathbf{max}\int F(\omega)\ d\omega \cong \sum_{1}^{[N]} \delta A_i \tag{25}$$

Therefore, while using small steps, the answer of optimization problem of critical excitation becomes

$$\mathbf{max}\quad f = \sum_{i=1}^{n} \sigma_{Di}^2 = \overline{s}\ \sum_{1}^{[N]} \delta A_i \tag{26}$$

3-1- Modified Optimization Method

A disadvantage of the ordinary method is its time-consuming inherent. In this method, for increasing the accuracy of the response and critical input excitation, it is required very large number of steps. Therefore, the ordinary method is inefficient, especially for the large structures. To overcome this disadvantage, a new method is presented. In the figure 7, it is seen that in the ordinary (old) method, ω_{1start} *and* ω_{1end} do not have equal $F(\omega)$. This nonoptimality is a result of dividing into equal $\delta\omega$'s.

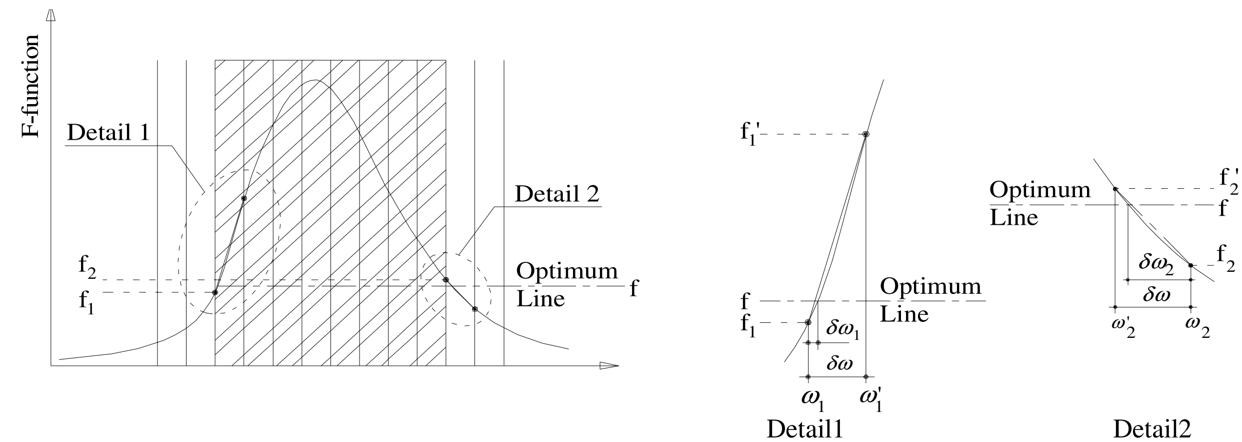

Fig. 7. *Modified Optimization Method*

To equalize F-functions of ω_{1start} *and* ω_{1end} and to produce an optimum line as shown in the fig 7, we can modify the start and the end frequencies (ω_1 *and* ω_2). By assuming the F-function to change linearly in each step $\delta\omega$, we have from details of figure 7 that

$$f = f_1 + m_1 \delta\omega_1 \qquad \text{(Detail 1)} \tag{27}$$

$$f = f_2 + m_2 \delta\omega_2 \qquad \text{(Detail 2)} \tag{28}$$

m$_1$ and *m*$_2$ are the slopes of the drawn line of details.Now, to include the decimal part, we have

$$--\delta\omega_1 + \delta\omega_2 = \left(\bar{S}/\bar{s}\right) - \left[\frac{\bar{S}/\bar{s}}{\delta\omega}\right]\delta\omega \tag{29}$$

The right term of the above equation is named $\delta\omega_r$. From equation (26), (27) and (28):

$$-\delta\omega_1 + \delta\omega_2 = \delta\omega_r \tag{30}$$

$$f_1 + m_1 \delta\omega_1 = f_2 + m_2 \delta\omega_2 \tag{31}$$

The equations (30) and (31) leads to

$$\delta\omega_1 = -\frac{\Delta f}{\Delta m} + \frac{m_2}{m_1 - m_2}\delta\omega_r \tag{32}$$

$$\delta\omega_2 = -\frac{\Delta f}{\Delta m} + \frac{m_1}{m_1 - m_2}\delta\omega_r \tag{33}$$

If $\delta\omega_r$ closes to zero, we have

$$\delta\omega_1 = \delta\omega_2 = -\frac{\Delta f}{\Delta m} \tag{34}$$

So the modified Area of F-function between the frequency bandwidth of input excitation is calculated

$$Modified\ \ Area = \sum A_i - \int_{\omega_1}^{\omega_1+\delta\omega_1} F(\omega)\ d\omega + \int_{\omega_2-\delta\omega_2}^{\omega_2} F(\omega)\ d\omega \tag{35}$$

Two integration in the equation (35) are taken by Simpson method. For MDOF systems that critical input excitation becomes two or more rectangles, the general equation becomes

$$\delta\omega_1 = \frac{\sum_{i=2}^{2n} \frac{f_i}{|m_i|} - f_1 \sum_{i=2}^{2n} \frac{1}{|m_i|} - \delta\omega_r}{1 + m_1 \sum_{i=2}^{2n} \frac{1}{|m_i|}} \tag{36}$$

In which, f_i *and* m_i are the *F*-function value and slope of the i^{th} Intersection of optimum line and *F*-function, respectively. Also, *n* is the number of frequency rectangles of critical input excitations. Now, other $\delta\omega_i$'s can be calculated

$$\delta\omega_i = \frac{1}{m_i}\left(f_1 - f_i + m_1\delta\omega_1\right) \tag{37}$$

5- EXAMPLES OF SDOF AND MDOF SYSTEMS

5-1- Single degree of freedom systems

In the SDOF systems, power spectral density of input excitation will be only one rectangle by the width of $\Delta\omega = \bar{S}/\bar{s}$. Accordingly, the mean square of the drift can be computed from

$$f = \sum_{i=1}^{n} \sigma_{Di}^2 = \bar{s} \int_{\omega_1}^{\omega_1+\bar{S}/\bar{s}} F(\omega)\ d\omega \tag{38}$$

Where

$$F(\omega) = H_D(\omega)\ \ H_D(-\omega) = \frac{1}{(\omega^2 - \omega_n{}^2)^2 + (2\xi\omega\omega_n)^2} \tag{39}$$

Authors in their last papers [4] presented the exact solution of optimal (maximal) story drift by taking partial differentiation of *f* relative to ω_1. Therefore, we had

$$\omega_{1max} = \omega_M Z - \frac{\Delta\omega}{2} \tag{40}$$

Where Z is modification factor near one and less than one.

$$Z = \sqrt{1 - (\frac{\Delta\omega/2}{\omega_M})^2} \tag{41}$$

In which ω_M is the peak value frequency of F-function and

$$\omega_M = \omega_n\sqrt{1 - 2\xi^2} \tag{42}$$

So the *f* -value becomes

$$f = \sum_{i=1}^{n} \sigma_{Di}^2 = \bar{s} \int_{\omega_{1max}}^{\omega_{1max}+\bar{S}/\bar{s}} F(\omega) d\omega \tag{43}$$

as an example, a SDOF example is considered. Its mass and stiffness is 25330 kg and 10^6 N/m . So the natural circular frequency and period becomes 6.283222 rad/s and 1 sec. In the exact method of optimization, Z-factor becomes 0.9141135 and critical excitation frequency range is calculated between 3.1879917 to 8.2704093 rad/sec as shown in figure 8 that comparing these numerical optimization methods with exact method verifies them. In the table 1, the result of the ordinary and modified methods are presented for different frequency steps ($\delta\omega$). In this table, it is seen that in the ordinary method, a large number of steps is needed to achieve a good accuracy in frequency bandwidth of critical excitation. For example, in the modified method, the input frequency bandwidth is calculated 3.18799 rad/sec to 8.27041 rad/sec which is more accurate than that of the ordinary method even with $\delta\omega = 10^{-3}$ that equals 3.188 to 8.270 rad/sec.

Table 1- Numerically optimized critical excitation for a SDOF system

$\xi = 0.05$ **Hyogoken-Nanbu, Kobe University NS, 1995**		$\delta\omega$ $(rad\,/\,\mathbf{sec}) =$		
		0.1	0.01	0.001
Ordinary Method of Optimization	$\omega_{1start} - \omega_{1end}$ =	3.2-8.2	3.19-8.2	3.188-8.27
	$Max(f) =$	0.118463591	0.1184657413	0.118465750433
Modified Method of Optimization	$\omega_{1start} - \omega_{1end}$ =	3.18142-8.26384	3.1879921-8.27041	3.187991730-8.27041
	$Max(f) =$	0.1184662312	0.11846575043	0.118465750749

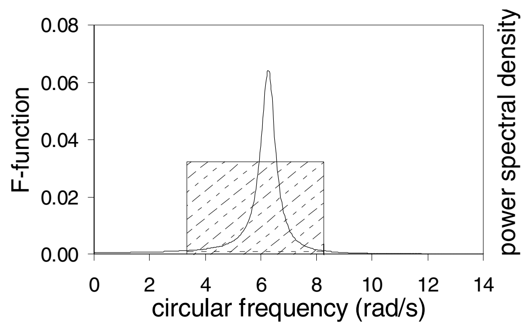

Fig. 8. *Optimal critical excitation of SDOF system with T=1 sec.*

5-2- Multi degree of freedom systems

In the figure 2 and 3, we saw three 2-DOF systems and their F-functions. In the figure 9, the optimal critical input excitation of the model1 (Ref. to Fig. 2) have been obtained. In the figure 9(a) and 9(b), the power and intensity limit are of El Centro NS (1940) and Hyogoken-Nanbu Kobe Univ. (1995), respectively. It is seen that the modal bandwidths of figure 9(b) is narrower than figure 9(a) because of the larger value of $\Delta\omega_{total}$ $(= Power\,/\,\, Intensity\,)$ for the earthquake of Hyogoken-Nanbu Kobe Univ. (1995). According to the figure 9, the bandwidth of the first mode is greater than the second mode for both earthquakes.

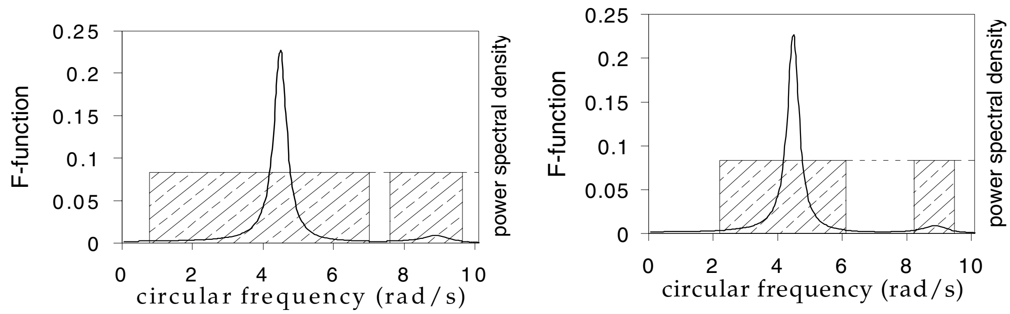

(a) (b)

Fig. 9. *Optimal critical excitation of Model1 (Ref. to Fig. 2)*

In the table 2, assuming different frequency steps ($\delta\omega$), the frequency bandwidthes and the *f*-value of the model1 (Ref. to Fig.2) to Hyogoken-Nanbu Kobe Univ. (1995) has been calculated. From this table, ordinary and modified optimization methods could be compared. It is seen that modified method needs fewer steps than ordinary method to achieve the same accuracy in calculating the start and end frequency bandwidthes and in calculating the objective fuction equals *f*-value.

Table 2- Numerically optimized critical excitation of Model1 for Hyogoken-Nanbu Kobe University, 1995

Model 1, $\xi = 0.05$ Hyogoken-Nanbu, Kobe University, 1995		$\delta\omega\ (rad/\mathbf{sec}) =$		
		0.1	0.01	0.001
Ordinary Method of Optimization	$\omega_{1start} - \omega_{1end} =$	2.2-6.1	2.210-6.110	2.207-6.107
	$\omega_{2start} - \omega_{2end} =$	8.2-9.30	8.17-9.35	8.1710-9.353
	$Max(f) =$	0.6320139466	0.63206448410	0.63206474727
Modified Method of Optimization	$\omega_{1start} - \omega_{1end} =$	2.20073-6.111756	2.206544-6.107456	2.206579088-6.10747544
	$\omega_{2start} - \omega_{2end} =$	8.1735227-9.3449153	8.1735227-9.3449153	8.171064-9.3525856
	$Max(f) =$	0.632069668	0.63206476985	0.63206475197

Also, the limits of El Centro NS (1940) is chosen and the same prolem is solved repitedly. The results are shown at the table 3. From this table, we can obtain the same results.
The total bandwidth ($\Delta\omega_{total}$) at the table 2 and 3 is equal to 8.424 and 5.082 for El Centro NS (1940) and Hyogoken-Nanbu Kobe Univ. (1995), respectively. Since the total bandwidth for both earthquakes is greater than $\Delta\hat{\omega}$ of model1, both of them yield two frequency bandwidthes as seen in the figure 9.

Table 3- Numerically optimized critical excitation of Model1 for El Centro NS, 1995

Model 1, $\xi = 0.05$ **El Centro NS, 1940**		$\delta\omega\ (rad/\mathbf{sec}) =$		
		0.1	0.01	0.001
Ordinary Method of Optimization	$\omega_{1start} - \omega_{1end} =$	0.6-6.9	0.54-6.90	0.537-6.901
	$\omega_{2start} - \omega_{2end} =$	7.5-9.6	7.52-9.58	7.525-9.585
	$Max(f) =$	0.668181179	0.668181179	0.668181179
Modified Method of Optimization	$\omega_{1start} - \omega_{1end} =$	0.5358-6.900	0.5362693-6.900934	0.536269297-6.9009026
	$\omega_{2start} - \omega_{2end} =$	7.522-9.582	7.5251391-9.584716567	7.52520534-9.58481446
	$Max(f) =$	0.668181179	0.668181179	0.668181179

Also, the Model2 is chosen as another model that has two besides peaks. Figure 10 showes the optimal critical input excitation of the mode2. It is seen that two frequency bandwidthes have joined together and only one frequency bandwidth have been produced. Table 4 shows the detailed results for different frequency steps.

Table 4- Numerically optimized critical excitation of Model2 for Hyogoken-Nanbu Kobe University, 1995

Model 2, $\xi = 0.05$ **Hyogoken-Nanbu, Kobe University,1995**		$\delta\omega\ (rad/\mathbf{sec}) =$		
		0.1	0.01	0.001
Ordinary Method of Optimization	$\omega_{1start} - \omega_{2end} =$	3.7-8.7	3.590-8.670	3.592-8.674
	$Max(f) =$	0.7375774	0.73758766	0.737587823
Modified Method of Optimization	$\omega_{1start} - \omega_{2end} =$	3.5888-8.6712	3.5917-8.67416	3.5918-8.674225
	$Max(f) =$	0.7375699	0.73758780	0.73758724

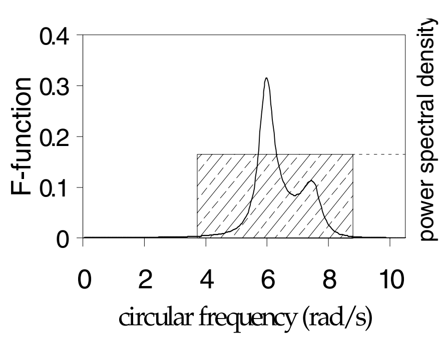

Fig. 10. *Optimal critical excitation of Model2 (Ref. to Fig. 2)*

As the last example, a four story building is considered with the modal frequencies equal to $\omega_1 = 5.42, \omega_2 = 8.84, \omega_3 = 12.65$ & $\omega_4 = 16.50 \quad rad/s$. we take $\delta\omega = 10^{-3}$ rad/s and the power and intensity of El Centro NS (1940) earthquake ($\bar{S} = 0.278 \quad , \bar{s} = 0.033$) as the limits. Then as shown in the figure 11, all the modal frequency bandwidthes have been calculated by the proposed method of optimization: $\Delta\omega_1 + \Delta\omega_2 = 7.024 \quad rad/s$, $\Delta\omega_3 = 1.400 \quad rad/s$ and $\Delta\omega_4 = 0$.

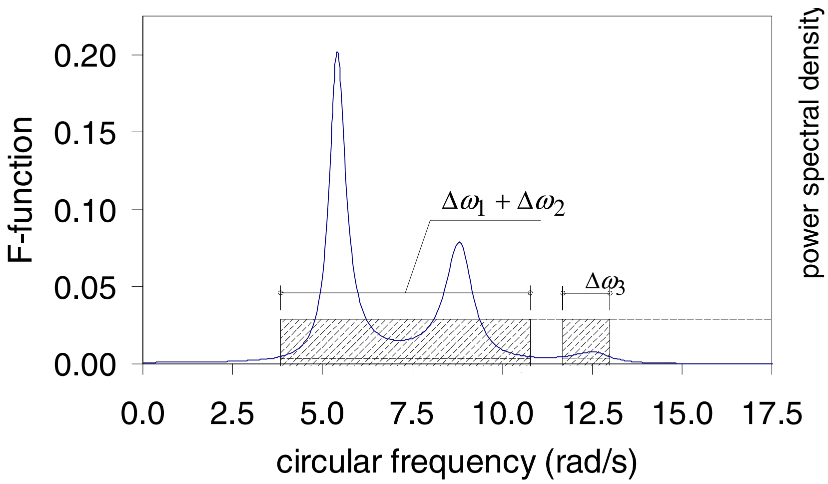

Fig. 11. *Critical excitation for 4-DOF system*

6-CONCLUSIONS

In this paper, ordinary method of finding optimal critical excitation has been modified. Comparing the modified and ordinary method shows the efficiency and speed of the proposed method specially for finding the start and end frequency of the modal bandwidthes. Multi degree of freedom examples show more effectiveness of the first modes than higher modes, especially for the narrowband input excitations and it is seen that if total frequency bandwidth ($\Delta\omega_{total}$) is less than an important frequency band ($\Delta\hat{\omega}$), only the first mode will be contributed.

REFERENCES

1. Drenick RF. "Model-free design of aseismic structures." Journal of Engineering Mechanics Division, ASCE 1970; 96(EM4):483-493

2. Shinozuka M. "Maximum structural response to seismic excitations." Journal of Engineering Mechanics Division, ASCE 1970; 96(EM5): 729-738.

3. Takewaki, I., "Optimal damper placement for critical excitation", Probabilistic Engineering Mechanics, 2000, Vol.15, No.4, pp. 317-325.

4. Ghodrati, G. and Ashtari, P. "Optimal Critical Excitation for Multi-story Buildings", Proceeding of 6th International Conference on Civil Engineering, Iran 2003, Vol. 6, pp 413-420

5. Ghodrati, G. and Ashtari, P. "Optimization Technique for Finding Probabilistic Critical Excitation", Proceeding of 7th International Conference on Probabilistic Safety Assessment and Management PSAM7, Berlin, 2004, accepted to be printed

6. Craig, R. R.," Structural Dynamics", John Wiley & Sons, 1982, New York